Journal of Sound and Vibration (1999) **222**(3), 505–511
Article No. jsvi.1998.1983, available online at http://www.idealibrary.com on IDEAL

AN ANALYSIS OF THE FLOW AND AERODYNAMIC ACOUSTIC SOURCES OF A CENTRIFUGAL IMPELLER

W.-H. Jeon and D.-J. Lee

Department of Aerospace Engineering, *KAIST*, *Kusong-dong*, *Yusong-gu*, *Taejon* 305-701, *Korea*

(*Received* 2 *June* 1998, *and in final form* 15 *September* 1998)

1. INTRODUCTION

Centrifugal fans are widely used due to their ability to achieve relatively high-pressure ratios in a short axial distance compared with axial fans. At the same time, the noise generated by these machines causes one of the most serious problems. In general, centrifugal fan noise is often dominated by tones at BPF (blade passage frequency) and its higher harmonics. This is a consequence of the strong interaction between the flow discharged from the impeller and the cut-off in the casing. To reduce these tones, many experiments have been performed [1, 2]. On the other hand, there is little research to predict the noise numerically because of the difficulty in obtaining detailed information about the flow field around the impeller and the casing [3]. Much research about the acoustic similarity law of a centrifugal fan with experimental data has been performed and now the similarity law is widely used [2, 4, 5]. The objective of this study is to understand the generation mechanism of sound and to develop a prediction method for the unsteady flow field and the acoustic field of a centrifugal fan. A discrete vortex method (DVM) is used to model the centrifugal fan and to calculate the flow field [6]. Lowson's method is used to predict the acoustic pressure in a free field [7]. In order to compare the experimental data, a centrifugal impeller and wedge introduced by Weidemann [4] are used in the numerical calculation and the results are compared with the experimental data.

2. NUMERICAL METHODS

Generally, a centrifugal fan is composed of three parts: an impeller, a diffuser and the casing. The impeller transforms the mechanical energy of the shaft to the kinetic energy of the flow, the diffuser recovers the pressure through a diffusing process and the casing collects and redirects the flow. The discrete tone noise is generated due to the interaction between the cut-off in the casing and the impeller. To simulate the noise generation, only an impeller and a wedge are chosen without the casing and these calculation results are compared with experimental ones (Figure 1). It is assumed that the impeller rotates with a constant angular velocity and the flow field of the impeller is incompressible and inviscid. The flow fields are calculated by the DVM described as follows. The impeller has NB number of blades and each blade has nc number of elements. Bound vortices are located at the 1/4 point of each element and control points are taken at the 3/4 point. Wake

0022–460X/99/180505 + 07 $30.00/0

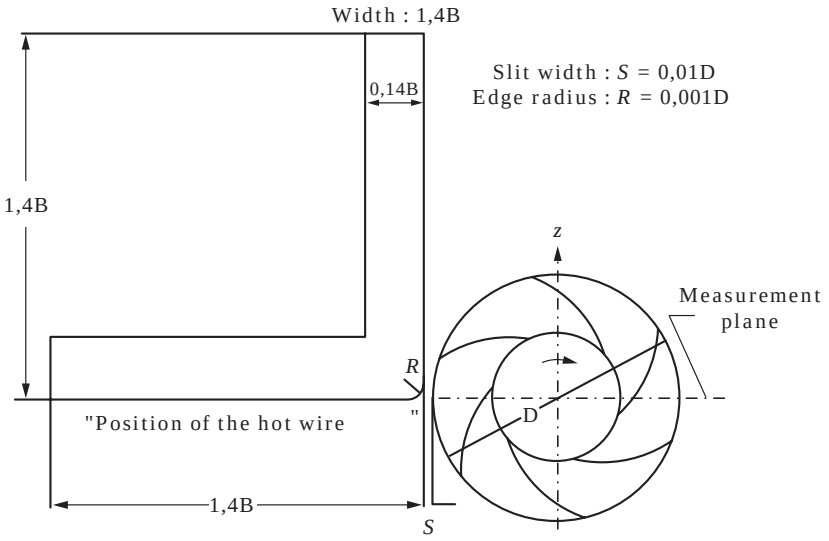

Figure 1. Dimensions of the impeller and wedge used by Weidemann.

vortices are shed at the trailing edge of the impeller at every time step to satisfy Kelvin's theorem. Shed vortices are convected with the local induced velocity. The inlet flow is modelled by a point source located at the center of the fan. The wedge is modelled with constant source panels where the control point is taken at the center of the element. The induced velocity at a point of the body ($\mathbf{x}_{cj}$) is as shown below.

$$\mathbf{U}(\mathbf{x}_c, t) = \mathbf{U}_Q(\mathbf{x}_c, t) + \mathbf{U}_{bv}(\mathbf{x}_c, t) + \mathbf{U}_{wv}(\mathbf{x}_c, t) + \mathbf{U}_{sp}(\mathbf{x}_c, t). \tag{1}$$

The first term on the right side represents the velocity at $\mathbf{x}_{cj}$ induced by the point source, the second term represents the velocity induced by bound vortices of the impeller, the third term represents the velocity induced by wake vortices and the fourth term represents the velocity induced by source panels. The shed vortices are convected with the local velocities.

The unknown strengths of the bound, the wake vortices and the source panels are calculated with the normal boundary condition that there is no flow across the surface boundary (equation (2)) and Kelvin's theorem (equation (3a)) [6].

$$[\mathbf{U}_Q(\mathbf{x}_c; t)_j + \mathbf{U}_{bv}(\mathbf{x}_c; t)_j + \mathbf{U}_{wv}(\mathbf{x}_c; t)_j + \mathbf{U}_{sp}(\mathbf{x}_c; t)_j] \cdot \mathbf{n}(\mathbf{x}_c)_j$$

$$= \begin{cases} \Omega(\mathbf{n}(\mathbf{x}_c)_j \times \mathbf{x}_{cj}(t)), & \text{impeller,} \\ 0, & \text{wedge,} \end{cases} \tag{2}$$

$$\frac{D\Gamma_m(t)}{Dt} = 0, \tag{3a}$$

$$\left[\sum_{k=1}^{nc} \Gamma_{bk}(t) + \sum_{k=1}^{nv} \Gamma_{wk}(t) \right]_m = 0. \tag{3b}$$

Here, Γ_m is the total circulation of that blade, composed of the circulation of bound vortices (Γ_b) of the impeller and shed wake vortices (Γ_w). And m, nc and nv denote the number of blades, the number of elements at one blade and the number of shed wake vortex particles, respectively.

The force of each element on the blade is calculated by the unsteady Bernoulli equation.

$$\mathbf{F}_{nj} = \rho\left\{\mathbf{U}(\mathbf{x}_c)\cdot\boldsymbol{\tau}_j\frac{\Gamma_{bj}}{\Delta s_j} + \frac{\partial}{\partial t}\sum_{k=1}^{j}\Gamma_{bk}\right\}\Delta s_j. \tag{4}$$

Here, $\mathbf{F}$, $\boldsymbol{\tau}$ and Δs_j are the normal force of the element, the tangential vector of the element and the length of that element.

In 1965, Lowson derived the formula of predicting the acoustic field generated by the moving point force from the wave equation [7]:

$$P - P_o = \left[\frac{x_i - y_i}{4\pi a_o r^2(1 - M_r)^2}\left\{\frac{\partial F_i}{\partial t} + \frac{F_i\,\partial M_r}{1 - M_r\,\partial t}\right\}\right]. \tag{5}$$

Here,

$$M_r = \frac{M_i r_i}{r}. \tag{6}$$

Equation (5) indicates that the acoustic pressure of the moving point force is calculated using the time variation of force and the acceleration. By applying this equation to each blade element, we can predict the acoustic pressure in a free field. The effects of the scattering and reflection due to the wedge are not considered. Only the behavior of the noise source and its radiation to the free field can be estimated.

3. ACOUSTIC SIMILARITY LAW

The first sound measurements concerned with similarity over a wide range of impeller sizes were made by Weidemann [4]. The general relationship among non-dimensional parameters developed by Weidemann may be written as follows:

$$\Delta\tilde{p}/P_o = Ma^{\alpha}Re^{\beta}F(St)G(He), \tag{7}$$

$$Re = \frac{UD}{\nu}, \qquad Ma = \frac{U}{a_o}, \qquad St = \frac{fD\pi}{UZ}, \qquad He = \frac{D}{\lambda}.$$

Here $\Delta\tilde{p}$, Ma, Re, St and He denote the r.m.s.-value of the predicted sound pressure, the Mach number of the flow, the Reynolds number, the Strouhal number and the Helmholtz number, respectively. U, D, a_o, Z represent the impeller tip velocity and the diameter of the impeller, speed of sound and the number of impeller blades, respectively.

The first two multipliers in equation (7) govern the influence of tip speed and impeller diameter, as well as the influence of viscosity. The function $F(St)$ describes the spectral distribution of the sound generated. Equation (7) implies that the

dependence on Mach number and Reynolds number is the same for all Strouhal numbers. The first three terms determine the generation of sound, since all of them depend on the rotor velocity. But $G(He)$ is a function of a purely geometric parameter: the ratio of impeller diameter to sound wavelength radiated. Therefore, $G(He)$ can be considered as an acoustic frequency response function which describes the sound radiation characteristics of the fan.

Values of 2·6 and 0·2 were found for the influence of Mach number (α) and Reynolds number (β) on the discrete frequency sound. In this numerical method, the exponent of the Mach number and $F(St)$ can be predicted, which are related to the sound generation.

4. NUMERICAL RESULTS

The centrifugal impeller with a rectangular wedge placed close to the impeller tip is used in the calculation. The impeller has six blades and rotates at $1200 \sim 4100$ rpm. The inlet diameter and inlet angle of the impeller are 0·112 m and 23·4°; the outlet diameter and outlet angle are 0·28 m and 33·5°. Numerical calculations of the flow field are conducted up to 30 non-dimensional times. One non-dimensional time means one revolution of the impeller. Figure 2 shows the variation of shed vortex strength at each blade in the 3000 rpm case. The strength of each wake vortex changes periodically and the pattern of each blade is similar. These changes of the strength cause the periodic change of the force at each blade element. Because of this unsteady rotating force of the impeller, discrete tones at BPF and higher harmonics are generated. Predicted acoustic signals are shown in Figure 3(b). In the spectrum not only the peak frequency but also the amplitude

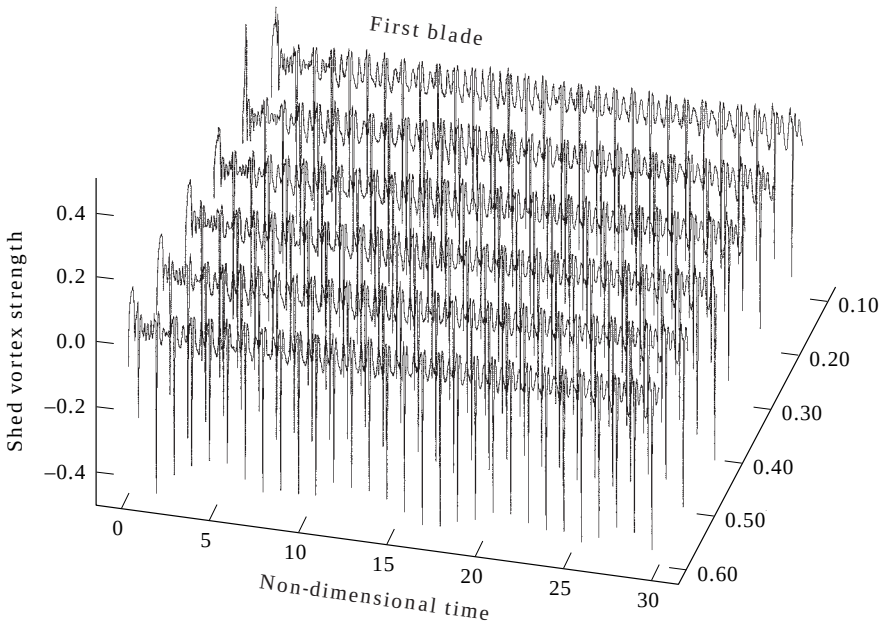

Figure 2. Variations of the shed vortex strength with time at each blade. (a) Measured spectrum [4]; (b) calculated spectrum (present calculation).

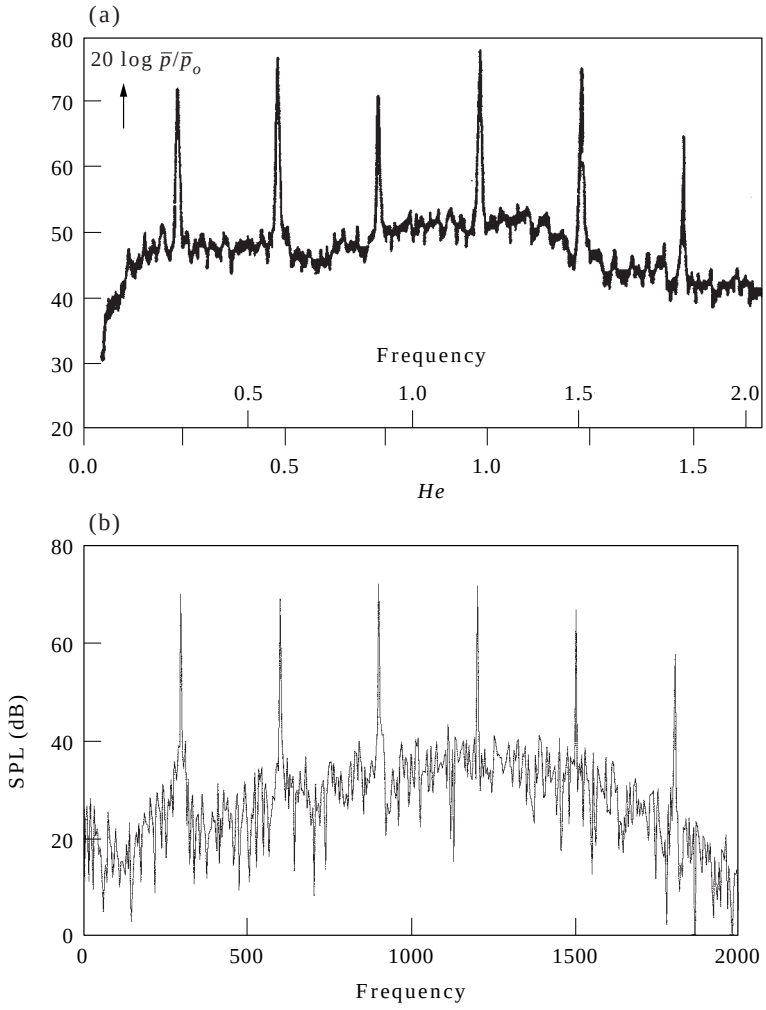

Figure 3. Comparisons of the frequency spectrum.

of the tonal sound are similar to the experimental data in Figure 3(a). The level of the blade passage frequency and its harmonics are much higher than the level of the broadband noise, because of the small gap distance between the impeller tip and the wedge. To verify the acoustic similarity law, other rpm cases are calculated. Here, the impeller tip velocity exponent, 2·8, is obtained from the calculation, which is the same value as Weidemann's result [4]. In Figure 4, the spectral distribution function, $F(St)$, of the experimental data and the calculated data are plotted. Note that $F(St)$ is different from zero only at integer values of the Strouhal number. The lines between integer values are meant only as a visual aid. The blade passage frequency is the most strongly excited, and there is a monotonic decrease as the Strouhal number increases. From Figure 4, the two lines are almost the same. This means that one can predict the sound generating mechanism of the centrifugal fan by using this method with agreeable accuracy.

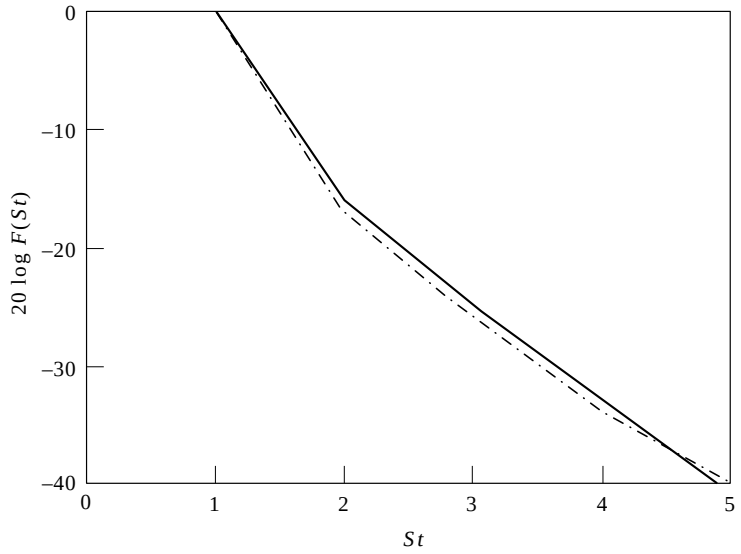

Figure 4. Comparison of the spectral distribution function with Weidemann's result. —, 20 log F (present calculation); – · – · , experiment (by Weidemann).

But the radiation effects like scattering, resonance and reflection are not considered. These effects are represented by $G(He)$ function in experiments.

From this calculation, it is confirmed that the source of blade passage frequency is an unsteady force fluctuation at impeller blades. This unsteady force fluctuation is generated by the periodic interaction of the impeller blade with the wedge.

5. CONCLUSIONS

The prediction method of identifying the noise source generated from a centrifugal fan has been developed. To predict the sound field, unsteady flow fields and unsteady force fluctuations are calculated by the DVM. Unsteady forces associated with the shed vortices at the blade tip are due to the interactions between the flow discharged from the impeller and the wedge.

The numerical results satisfy the acoustic similarity law formulated by Weidemann. Furthermore, the impeller tip velocity exponent for the sound pressure is in good agreement with the experimental value. Also the calculated spectral distribution function of sound generated from the fan is similar to the experimental value. This means that the numerical method used in this paper can predict the aeroacoustic source of a centrifugal impeller with good accuracy.

ACKNOWLEDGMENT

This work was partially supported by the Agency for Defense Development.

REFERENCES

1. R. C. CHANAUD 1973 *Journal of Acoustical Society of America* **37**, 969–974. Aerodynamic sound from centrifugal-fan rotors.

2. W. Neise 1975 *Journal of Sound and Vibration* **43**, 61–75. Application of similarity laws to the blade passage sound of centrifugal fans.
3. W.-H. Jeon, D.-J. Lee 1997 *The 5th International Congress on Sound and Vibration*. An analysis of the flow and sound source of an annular type centrifugal fan.
4. J. Weidemann 1971 *NASA TT F*-13, 798. Analysis of the relation between acoustic and aerodynamic parameters for a series of dimensionally similar centrifugal fan rotors.
5. L. Mongeau, D. E. Thompson and D. K. McLaughlin 1993 *Journal of Sound and Vibration* **163**, 1–30. Sound generation by rotating stall in centrifugal turbomachines.
6. M. Kiya 1988 *Soviet Union–Japan Symposium on Computational Fluid Dynamics*. Discrete vortex simulation of separated unsteady flow in a centrifugal impeller.
7. M. V. Lowson 1965 *Proceedings of the Royal Society in London*, *Series A* **286**, 559–572. The sound field for singularities in motion.